RSC Advances

ROYAL SOCIETY OF CHEMISTRY

www.rsc.org/advances

Nitrogen functional groups on activated carbon surface for the effect of the ruthenium catalysts in acetylene hydrochlorination

Na Xu[a], Mingyuan Zhu* [a, b], Jinli Zhang* [a, c], Haiyang Zhang [a, b], Bin Dai[a, b]

[a]School of Chemistry and Chemical Engineering of Shihezi University, Shihezi, Xinjiang, 832000, PR China.

[b]Key Laboratory for Green Processing of Chemical Engineering of Xinjiang Bingtuan, Shihezi, Xinjiang, 832000, PR China.

[c]School of Chemical Engineering and Technology, Tianjin University, Tianjin, 300072, PR China.

*Corresponding author. Tel.: +86 993 2057270; Fax: +86 993 2057210.

E-mail address: zhuminyuan@shzu.edu.cn (M. Zhu)

*Corresponding author. Tel.: +86-22-27890643; Fax: + 86-22-27890643.

E-mail address: zhangjinli@tju.edu.cn (J. Zhang)

Abstract To improve the activity and stability of Ru-based catalysts with the carbon support for acetylene hydrochlorinatio, activated carbon was consecutively modified with nitration, amination and pyridine, and the effect of different carbon supports on Ru-based catalysts for acetylene hydrochlorination was investigated. The result of FT-IR confirmed that $-NO_2$, $-NH_2$ and -N-H-N were separately grafted onto the surface of AC. Under the same reaction conditions, the modified catalysts exhibit better catalytic activity compared with the original Ru/AC catalyst. Moreover, the catalyst Ru/AC-NHN shows the best catalytic performance with a slightly decrease after 48 h from 93.2% to 91.8%. The increase in catalytic activity indicates that the modification of nitrogen function groups is beneficial for acetylene hydrochlorination.

Keywords: activated carbon; nitration modification; ammoniation modification; Ru-based catalyst; acetylene hydrochlorination.

1. Introduction

Acetylene hydrochlorination reaction is the important process to synthesize vinyl chloride in the industry. However, the catalyst used in the reaction is the $HgCl_2$ catalyst, which has the defect of highly toxic and serious environmental pollution. Therefore, it is imperative to explore non-mercury catalysts with high activity and long stability for acetylene hydrochlorination.

The pioneer works of Hutchings suggested that the activity of metal catalysts were associated with the standard electrode potentials of the related metal ions [1]. Accordingly, $AuCl_3$ catalyst is the optimal catalyst with its high activity. In fact, whereas Ru is also precious metal, it is the low-cost compared to Au, and Ru-based catalysts have been caused extensive research. However, the catalytic activity and stability of the Ru-based catalysts still need to be further improved in the acetylene hydrochlorination process. Bimetallic Ru-Co/SAC resulted in good catalytic activity and coking inhibition capability [2]. Li et al. reported that Ru catalysts deposited inside the CNTs channels exhibited the optimal catalytic activity, with the acetylene conversion of 95.0% and the selectivity to VCM of 99.9% [3]. Additionally, Pu et al. reported that the original Ru/SAC catalyst was oxidized under air at 300 °C for 1 h with the catalytic performance of stable acetylene conversion at 96.5% in 48 h at 170 °C and C_2H_2 gas hourly space velocity (GHSV) of 180 h^{-1} [4].

In the field of acetylene hydrochlorination, activated carbon is the best catalyst carrier. According to the previous report, the functional groups on activated carbon surface will affect its catalytic activity. Recently, Zhao et al. had successfully

demonstrated that the doping of nitrogen can efficiently enhance the catalytic performance of Au/AC and Au-Cs/AC [5-6]. Wang et al. reported that the P-doped carbon support can also significantly enhance the catalytic activity of Au/SAC catalyst for acetylene hydrochlorination [7]. Previous literature also reported that amino-functionalized metal-organic frameworks adsorbed pyridine via hydrogen bonding [8]. According to the understanding of previous knowledge, there are no reports of amination of activated carbon with pyridine with hydrogen bonding for acetylene hydrochlorination.

Therefore, in this work, we prepared Ru-based catalysts supported on activated carbon, which was modified with -NO_2, -NH_2 and -N-H-N, and assessed the catalytic activity for acetylene hydrochlorination, aiming to improve the activity and stability of acetylene hydrochlorination. In combination with characterizations of TEM, TPR, XPS and FT-IR, etc., it was indicated that Ru-based catalyst deposited on activated carbon modified by -N-H-N exhibited the highest catalytic activity for acetylene hydrochlorination.

2. Experimental

2.1. Materials

Activated carbon (neutral, coconut carbon) was purchased from Tangshan United Carbon Technology Co., Ltd; $RuCl_3$ (with 48.7% Ru content) and nitric acid (AR, 65.0%-68.0%) were purchased from Tianjin Fengchuan Chemical Reagent Technology Co., Ltd; acetic anhydride (AR, ≥98.5%) was purchased from Tianjin Yongsheng Chemical Reagent Co., Ltd; pyridine (AR, ≥99.5%) was purchased from

Tianjin Fuyu Fine Chemical Co., Ltd; aqua ammonia (AR, 25.0%-28.0%) and sodium borohydride (AR, ≥97.0%) were purchased from Chengdu Kelong Chemical Reagent Company. All the other materials and chemicals were commercially available and were used without further purification.

2.2. Modification of AC samples

According to the previously reported method [9], nitration modification of the AC sample was performed as follows: 30 ml of nitric acid was slowly dripped into a suspension of AC and 40 ml acetic anhydride in a three neck round bottom flask at room temperature. After stirring at this temperature for 24 h, the solid sample was filtrated and washed until the filtrate was neutral. The sample was dried at 110 °C for 14 h, and labeled as AC-NO_2.

Amination of the AC-NO_2 sample was carried out as follows: AC-NO_2 was mixed with 10 ml of ammonia solution and 20 ml of deionized water. After adding 0.75g of sodium borohydride, the suspension was kept at room temperature for 24 h under stirring. The solid was filtrated, washed with deionized water until the filtrate was neutral, and then dried at 110 °C for another 24 h. The obtained sample was labeled as AC-NH_2.

Then 20 ml of pyridine was dripped into AC-NH_2 in a three neck round flask at room temperature. After stirring at this temperature for 24 h, the solid samples were filtrated and washed until the filtrate was neutral, and then dried at 110 °C for 14 h. The obtained sample was labeled as AC-NHN.

2.3. Preparation of Ru-based catalysts

Ru-based catalysts were prepared via the incipient wetness impregnation method [10]. A $RuCl_3$ aqueous solution was quantitatively mixed with the modified carbon support under stirring to prepare the catalyst with Ru loading content of 1 wt%. Then it was desiccated at 140 °C for 18 h. The obtained catalysts were labeled as Ru/AC, Ru/AC-NO_2, Ru/AC-NH_2 and Ru/AC-NHN, respectively.

2.4. Catalyst characterization

Low temperature N_2 adsorption-desorption experiment was performed with a Micromeritics ASAP 2020 instrument to investigate surface area and porosity. The Fourier-transform infrared spectroscopy (FT-IR) was used to judge functional group changes with Harrick's Praying Mantis diffuse reflection attachment. Transmission electron microscopy (TEM) was performed with a JEM2010 electron microscope at an accelerating voltage of 200 kV. X-ray diffraction (XRD) patterns were collected using a Bruker D8 advanced X-ray diffractometer with Cu-Kα irradiation (λ= 1.5406 Å) at 40 kV and 40 mA at wide angles (10-90^o in 2θ). Temperature-programmed reduction (TPR) measurement was performed using a TPDRO 1100 (Thermo-Finnigan) instrument equipped with a thermal conductivity detector (TCD). The weight of the tested samples was 100mg. Prior to each test, the samples were treated with N_2 gas at 60 °C for 1 h. After cooling, the temperature was increased from 30 to 800 °C at a heating rate of 10 °C min^{-1} with a 10.0% H_2/Ar atmosphere flowing at a rate of 40 mL min^{-1}. Temperature-programmed desorption (TPD) was also analyzed by TPDRO 1100 apparatus at a temperature ramp of 25–400 °C with a ramp rate of 10 °C min^{-1} and a flow rate of 45 mL min^{-1}, the final temperature of

400 °C was maintained for 20 min. X-ray photoelectron spectroscopy (XPS) data using an Axis Ultra spectrometer were recorded using an Axis Ultra spectrometer equipped with a monochromatized Al-Kα X-ray source (225 W).

2.5. Catalytic performance tests

The catalytic performance tests for acetylene hydrochlorination were carried out in the fixed-bed reactor (i.d., 10 mm). A purge pipeline with nitrogen was used prior to the catalytic reaction to remove water and air in the system. Then the catalyst (2 mL) was activated with hydrogen chloride (gas, 99%) at a flow rate of 20 mL min^{-1}. After the reactor was heated to 180 °C, acetylene (11.8 mL min^{-1}) and hydrogen chloride (13.5 mL min^{-1}) were fed through the heated reactor to achieve a GHSV (C_2H_2) of 360 h^{-1}, which contained 2 mL of catalyst. The reaction products were analyzed by gas chromatography (GC-2014C).

3. Results and Discussion

The catalytic performance of the catalysts and the supports are shown in Fig. 1. It can be seen that the supports (AC, AC-NO_2, AC-NH_2 and AC-NHN) exhibit relatively low activity for the acetylene hydrochlorination (Fig. 1a). Compared with the original Ru/AC catalyst, the catalytic activity and stability of the Ru-based catalysts (Ru/AC-NO_2, Ru/AC-NH_2 and Ru/AC-NHN) are greatly enhanced when AC is modified with nitrogen functional groups, and the initial acetylene conversion increases as activated carbon is decorated consecutively, achieving the highest value of 93.2% over Ru/AC-NHN catalyst with no obvious decline after 48 hours' reaction. All these related catalysts show the selectivity to VCM above 99.0% at 48 h (Fig. 1b

and d). This result indicates that the presence of nitrogen functional groups, especially the –NHN, promotes the initial catalytic activity of the Ru-based catalysts and significantly enhances the catalyst stability.

The FT-IR spectra of the supports AC, AC-NO_2, AC-NH_2 and AC-NHN are shown in Fig. 2. Compared with AC, AC-NO_2 shows a characteristic peak at 1328 cm^{-1}, which is assigned to the fundamental vibration of -NO_2 group [11]. However, the peak disappears after further amination of the AC-NO_2, and for the AC-NH_2, the peaks at 3744 and 1521 cm^{-1} are assigned to the vibration of NH_2 and NH in the amine groups, respectively [12]. Further, the characteristic peak of NH has a shift to lower wavelengths (1508 cm^{-1}) and a new peak at 2987 cm^{-1} appears in the AC-NHN. This is probably due to the action of hydrogen bonding formed by accepting a proton from NH_2 and forming a strong hydrogen bond with pyridine [13]. Thus, the FT-IR results confirm that the nitrogen functional groups (-NO_2, -NH_2 and -NHN) were successfully grafted onto the surface of AC in the consecutive amination steps.

Elemental analysis is carried out to determine the amount of nitrogen-containing groups grafted onto activated carbon surface, the results are listed in Table 1. Only a trace amount of nitrogen is detected on AC, which is possibly originated from weekly physisorbed nitrogen impurities on the surface [14]. Then the content of nitrogen increases gradually from 0.73% for AC-NO_2 to 1.67% for AC-HNH as the activated carbon was consecutively modified, indicating the presence of nitrogen-containing functional groups. Table 2 shows the specific surface area and total pore volume of the support AC before and after surface modification. The BET surface areas for AC,

AC-NO_2, AC-NH_2 and AC-HNH are 1030, 871, 933 and 924 m^2 g^{-1}, respectively. The pore volumes of AC, AC-NO_2, AC-NH_2 and AC-HNH are 0.57, 0.44, 0.52 and 0.51 cm^3g^{-1}, respectively. The decrease in BET surface areas and pore volumes may also indicate that the functional groups were successfully grafted on the surface of AC and the pores were occupied by these group after surface modification [15-16].

Fig. 3 indicates the XRD patterns of AC, the fresh catalysts Ru/AC, Ru/AC-NO_2, Ru/AC-NH_2 and Ru/AC-NHN. As shown in Fig. 3, apart from two obvious diffraction peaks at 23.4^0 and 43.5^0 originating from the (002) and (101) planes of AC, no discernible reflection of metallic Ru or anhydrous tetragonal RuO_2 is detected for all the catalysts[17], indicating the high dispersion of active species or small particle size (< 4 nm) [18]. In addition, the TEM images in Fig. 4 show that it is difficult to distinguish the homogeneous dispersion of small and uniform Ru particles. This may be due to the high dispersion of the Ru particles, which is consistent with the XRD results. Moreover, the dispersion of Ru elements was estimated by the CO chemisorption experiments [19]. As listed in Table 3, the Ru dispersion is 80.58% for the Ru/AC catalyst. However, the Ru dispersion decreases after the modification of the nitrogen functional groups, with the lowest dispersion of 45.53% achieved in Ru/AC-NHN catalyst, followed by Ru/AC-NH_2 (51.17%) and Ru/AC-NO_2 (68.04%). Thus, the modifications of actived carbon is not beneficial to improve the dispersion of the catalysts.

TGA analysis is carried out to obtain the amount of carbon deposition, and the results are shown in Fig. 5. In the case of the Ru/AC-HNH catalyst, both the fresh and

used catalysts have a slight weight loss before 150 ℃ owing to the desorption of adsorbed water (Table S1). In the temperature range of 150-400 ℃, there is an obvious weight loss (10.0%, Table S1) on the used catalysts under the atmosphere. When the temperature exceeds 400 ℃, there appears a rapid weight loss mainly due to the combustion of activated carbon. Thus, the coke burning may occur in the temperature range of 150–400 ℃. Taking into account the AC support can lose its weight by reacting with oxygen to emit CO_2, the amount of carbon deposition is calculated by the difference of the weight loss between the fresh and the used catalysts in the temperature range of 150–400 ℃ [20-22]. Based on Fig. 5, the amount of carbon deposition on the used Ru/AC-HNH catalyst is calculated as 1.9%.

Similarly, the carbon deposition on other used catalysts were also calculated via the corresponding TG and DTG curves (Fig. S1). As listed in Table 4, for the Ru-based catalysts, the amount of carbon deposition increases in the order: Ru/AC-NHN(1.9%) < Ru/AC-NH_2 (3.2%) < Ru/AC-NO_2(6.8%) < Ru/AC (13.2%). It is clearly indicated that the AC modified by nitrogen functional groups can greatly prevent the coking deposition of the Ru catalyst.

Fig. 6 displays the TPR profiles of the supports and Ru-based catalysts. The broad peak in the range of 500–700 ℃ for all the samples is attributed to the reduction of oxygenated groups in the carbon support. For the supports AC-NO_2, there is a weak reduction peak appeared in the temperature range of 350–480 ℃, which corresponds to the characteristic reduction band of –NO_2. However, there are no obvious peaks appeared in the same temperature range for the other modified carriers. Obviously,

there are some H_2 consumption peaks in the temperature range of 100–400 °C for all the Ru-based catalysts, which are due to the reduction of ruthenium species involving the ruthenium oxides and ruthenium chloride in the catalysts. Specifically, for the Ru/AC catalyst, the peak at 138 °C is attributed to the reduction of $RuCl_3$ [23]. For the Ru/AC-NO_2 catalyst, there exhibits a shoulder peak at 299 °C and a strong peak at 323 °C attributed to the reduction of Ru^{n+} ($n \geq 4$) species [24]. While for Ru/AC-NH_2 catalyst, there are two peaks at 202 °C and 293 °C, which correspond to the reduction peak of $RuCl_3$ and RuO_2, respectively [25-26]. The catalyst of Ru/AC-NHN shows a broad peak corresponded to RuO_2 at 291 °C. Through comparing the TCD signals with a standard, it can be estimated that the fraction of different Ru species existed in these fresh catalysts. Calculated from the peak area of TPR, it is worth mentioning that the relative amounts of H_2 consumption peaks reduces in the order: Ru/AC (4.16%) < Ru/AC-NH_2 (6.64%) < Ru/AC-NHN (20.60%) < Ru/AC-NO_2 (68.60%) (Table 5). It is suggested that there may exist interaction between the active species and supports to influence the content of the ruthenium species with different variation.

To explore the amount and kind of the ruthenium species, XPS deconvolution of Ru 3p3/2 (Figs. 2 and 3 in Supporting Information) is measured to distinguish different species, including their binding energy and relative quantity. For both the fresh and used Ru-based catalysts, Ru XPS spectra were deconvoluted into four peaks at 461.86 eV, 463.52 eV, 465.04 eV and 466.45 eV, corresponding to the species of metallic Ru, $RuCl_3$, RuO_2 and RuOx, respectively [27-29]. Table 6 shows the ruthenium species and their relative amounts in the fresh and used Ru-based catalysts.

For the fresh Ru/AC, it consists of 50.52% $RuCl_3$, 18.69% RuO_2, 16.35% RuO_x, 14.44% metallic Ru. For the fresh Ru-based catalysts deposited on activated carbon modified by nitrogen functional groups, the content of RuO_2 is clearly higher than that of the fresh Ru/AC. The previous work demonstrated that RuO_2 is the important active ingredient in acetylene hydrochlorination. The carbon modified by nitrogen functional groups can influence the performance of the resultant catalysts, due to enhanced π bonding in the framework, and promote their electron donor-acceptor properties. However, the detailed reaction mechanism is yet to be explored in the future work.

Fig. 7 shows the HCl- and C_2H_3Cl- TPD profiles of Ru-based catalysts. The desorption area corresponds to the adsorption amount of adsorbed species on the catalysts, and the desorption temperature reflects the adsorption strength. As seen in Fig. 7a, HCl desorption peak areas on the Ru-based catalysts loaded on modified activated carbon are larger than those on Ru/AC, while the corresponding desorption temperature are slightly higher. Fig. 7b shows the desorption of C_2H_3Cl on the Ru-based catalysts. The peak area on Ru/AC-NHN is the smallest compared with other catalysts, which is beneficial to the acetylene hydrochlorination reaction. This indicates that the catalysts loaded on the modified activated carbon show enhanced adsorption of hydrogen chloride and waning vinyl chloride, which promotes higher catalytic activities for the acetylene hydrochlorination reaction (Fig. 1c).

4. Conclusion

Ru-based catalysts with different supports are prepared using the incipient wetness

impregnation method. To study the change of AC modified with nitrogen function groups and the effects on Ru-based catalysts, those characterization of XRD, BET, TEM, FT-IR, TPD, TPR and XPS are used. XPS analysis reveals that carbon supports modified by nitrogen functional groups can affect the amount of ruthenium species in the catalysts involved in metallic Ru, $RuCl_3$, RuO_2 and RuOx, which results in good catalytic activity. The best catalytic performance is achieved over the catalyst Ru/AC-NHN, which is a promising non-mercuric catalyst for acetylene hydrochlorination. The increase in catalytic activity indicates that the modification of nitrogen functional groups will be beneficial for acetylene hydrochlorination.

Acknowledgments

This work is supported by the National Basic Research Program of China (973 Program, 2012CB720302), National Natural Science Funds of China (NSFC, U1403294, 21366027), Young Scientific and Technological Innovation Leader of Bingtuan (2015BC001), and the Foundation of Young Scientist in Shihezi University (No. 2013ZRKXJQ03).

References

[1] G. J. Hutchings, J. Catal., 1985, 96, 292-295.

[2] J. Zhang, W. Sheng, C. Guo and W. Li, RSC. Adv., 2013, 3, 21062-21068.

[3] G. Li, W. Li, H. Zhang, Y. Pu, M. Sun and J. Zhang, RSC. Adv., 2015, 5, 9002-9008.

[4] Y. Pu, J. Zhang, L. Yu, Y. Jin, W. Li, Appl. Catal., B, 2014, 488, 28-36.

[5] J. Zhao, J. Xu, J. Xu, T. Zhang, X. Di, J. Ni, X. Li, Chem. Eng. J., 2015, 262, 1152–1160.

[6] J. Zhao, T. Zhang, X. Di, J. Xu, J. Xu, F. Feng, J. Ni, X. Li, RSC. Adv., 2015, 5, 6925-6931.

[7] B. Wang, L. Yu, J. Zhang, Y. Pu, H. Zhang, W. Li, RSC. Adv., 2014, 4, 15877-15885.

[8] Z. Hasan, M. Tong, B. K. Jung, I. Ahmed, C. Zhong, S.H. Jhung, J. Phys. Chem. C., 2014, 118, 21049−21056.

[9] H. Cao, L. Xing, G. Wu, Y. Xie, S. Shi, Y. Zhang, D. Minakatad, J. C. Crittenden, Appl. Catal., B, 2014, 146, 169-176.

[10] B. Nkosi, M. D. Adams, N. J. Coville, G. J. Hutchings, M. D. Adams, J. Friedl, F. E. Wagner, J. Catal., 1991, 128, 366-377.

[11] E. Bekyarova, M. E. Itkis, P. Ramesh, C. Berger, M. Sprinkle, W. A. de Heer, R. C. Haddon, J. Am. Chem. Soc., 2009, 131, 1336-1337.

[12] V. Jaiboon, B. Yoosuk, P. Prasassarakich, Fuel Processing Technology, 2014, 128, 276-282.

[13] T. Noguchi, BBA., 2014, 1847, 35-45.

[14] M. Yang, T. Yang, M. Wong, Thin Solid Films., 2004, 1, 469-470.

[15] C. Moreno-Castilla, M.A. Ferro-Garcia, J.P. Joly, I. Bautista-Toledo, F. Carrasco-Marin, J. Rivera-Utrilla, Langmuir., 1995, 11, 4386-4392.

[16] I. Bautista-Toledo, J. Rivera-Utrilla, M.A. Ferro-Garcia, C. Moreno-Castilla, Carbon, 1994, 32, 93-100.

[17] H. Qian, F. Han, B. Zhang, Y. Guo, J. Yue, B. Peng, Carbon., 2004, 42, 761-766.

[18] P. Gao, A. Wang, X. Wang and T. Zhang,Catal. Lett., 2008,125, 289 – 295.

[19] Y. Li, G. Lan, G. Feng, W. Jiang, W. Han, H. Tang and H. Liu, Chem Cat Chem, 2014, 6, 572-579.

[20] S. Wang, B. Shen, Q. Song, Catal. Lett., 2009, 134, 102-109.

[21] L. Wang, F. Wang, J. Wang, 2015, 65, 41-45.

[22] H. Zhang, B. Dai, X. Wang, W. Li, Y. Han, J. Gu and J. Zhang,Green Chem., 2013, 15, 829-836.

[23] V. Mazzieri, F. Coloma-Pascual, A. Arcoya, P. C. L'Argentière, N. S. Fígoli, Appl. Surf. Sci., 2003, 210, 222-230.

[24] F. Li, J. Chen, Q. Zhang and Y. Wang, Green Chem., 2008, 10, 553.

[25] S. Guo, X. Pan, H. Gao, Z. Yang, J. Zhao and X. Bao, Chem. Eur. J., 2010, 16, 5379-5384.

[26] P.G.J. Koopman, A.P.G. Kieboom, H. van Bekkum, J. Catal., 1981, 69, 172-179.

[27] J. L. Gómez de la Fuente, M. V. Martínez-Huerta, S. Rojas, P. Hernández-Fernández, P. Terreros, J. L. G. Fierro, M. A. Peña, Appl. Catal. B.

Environ., 2009, 88, 505-514.

[28] S. Sharma, Z. Hu, P. Zhang, E. W. McFarland, H. Metiu, J. Catal., 2011, 278, 297-309.

[29] J. -H. Ma, Y. -Y. Feng, J. Yu, D. Zhao, A. -J. Wang, B. -Q. Xu, J. Catal., 2010, 275, 34-44.

Figure Captions:

Fig.1 Acetylene conversion (a,c) and selective (b,d) to VCM over the supports and the catalysts. Reaction conditions: Temperature (T) = 180 °C, GHSV (C_2H_2) = 360 h^{-1}, V (HCl)/V (C_2H_2) =1.15.

Fig.2 FT-IR spectra of: (a) AC, (b) AC-NO_2, (c) AC-NH_2, (d) AC-NHN.

Fig.3 X-ray diffraction patterns of (a) the support AC and the fresh catalysts (b) Ru/AC, (c) Ru/AC-NO_2, (d) Ru/AC-NH_2 and (e) Ru/AC-NHN.

Fig.4 TEM images of the fresh catalysts: (a) Ru/AC, (b) Ru/AC-NO_2, (c) Ru/AC-NH_2 , and (d) Ru/AC-NHN.

Fig.5 TGA curves of the fresh and used catalysts of Ru/AC-NHN.

Fig.6 TPR profiles of the supports: (a) AC, (b) AC-NO_2, (c) AC-NH_2, (d) AC-NHN and the catalysts: (a) Ru/AC, (b) Ru/NH_2, (c) Ru/AC-NHN, and (d) Ru/AC-NO_2.

Fig.7 TPD evolution profiles of Ru-based catalysts: (a) HCl- and (b) C_2H_3Cl-.

Table 1
Elemental analysis for the supports.

Sample	Element Composition (%)		
	C	H	N
AC	85.99	3.36	0.21
AC-NO_2	78.77	3.59	0.73
AC-NH_2	80.88	3.82	1.05
AC-NHN	82.57	3.51	1.67

Table 2
Physical properties of different AC samples.

Samples	$S_{BET}(m^2g^{-1})$	$V(cm^3g^{-1})$	D(nm)
AC	1030	0.57	2.20
AC-NO_2	871	0.44	2.01
AC-NH_2	933	0.52	2.25
AC-NHN	924	0.51	2.21

S_{BET}: surface area; V: total pore volume; D: average pore diameter.

Table 3
Estimated Ru element dispersion in the catalysts determined by CO chemisorption.

Catalysts	CO uptake (μmol CO/g)	Ru dispersion (%)
Ru/AC	76.54	80.58
Ru/AC-NO_2	63.95	68.04
Ru/AC-NH_2	50.12	51.17
Ru/AC-NHN	43.70	45.53

Table 4
Carbon deposition of Ru-based catalysts.

Catalysts	Content of carbon deposition (%)
Ru/AC	13.2
Ru/AC-NO_2	6.8
Ru/AC-NH_2	3.2
Ru/AC-NHN	1.9

Table 5
The relative amounts of H_2 consumption peaks in the catalysts.

Catalysts	H_2 consumption peaks (%)
Ru/AC	4.16
Ru/AC-NO_2	68.60
Ru/AC-NH_2	6.64
Ru/AC-NHN	20.60

Table 6
The relative content and binding energy of ruthenium species in the fresh catalysts.

Sample	Area%,Binding energy(eV)			
	Ru	$RuCl_3$	RuO_2	RuO_x
Fresh Ru/AC	461.86(14.44)	463.52(50.52)	465.04(18.69)	466.45(16.35)
Fresh Ru/AC-NO_2	461.53(3.95)	463.22(40.24)	464.83(31.19)	466.70(24.62)
Fresh Ru/AC-NH_2	462.10(13.32)	463.43(47.30)	465.08(30.37)	466.66(9.01)
Fresh Ru/AC-NHN	461.67(9.96)	463.13(35.04)	464.71(40.22)	467.03(14.78)
Used Ru/AC	461.31(21.10)	463.18(46.51)	464.72(17.44)	466.59(14.95)
Used Ru/AC-NO_2	461.45(31.88)	463.14(33.66)	464.48(28.50)	466.16(5.96)
Used Ru/AC-NH_2	462.85(24.70)	463.78(40.38)	465.15(24.09)	466.88(10.83)
Used Ru/AC-NHN	462.15(17.69)	463.30(33.27)	464.65(35.03)	466.12(14.01)

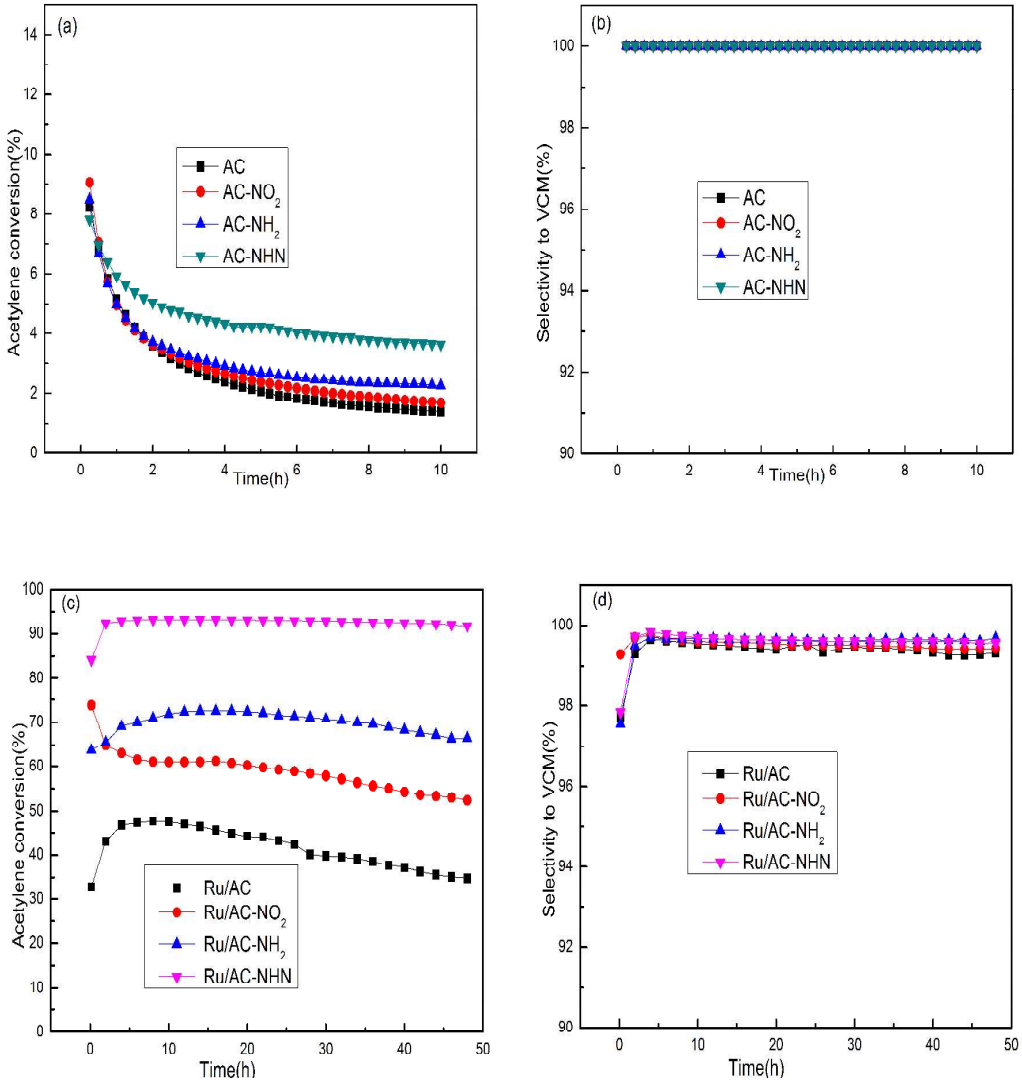

Fig.1 Acetylene conversion (a,c) and selective (b,d) to VCM over the supports and the catalysts. Reaction conditions: Temperature (T) = 180 °C, GHSV (C_2H_2) = 360 h^{-1}, V (HCl)/V (C_2H_2) =1.15.

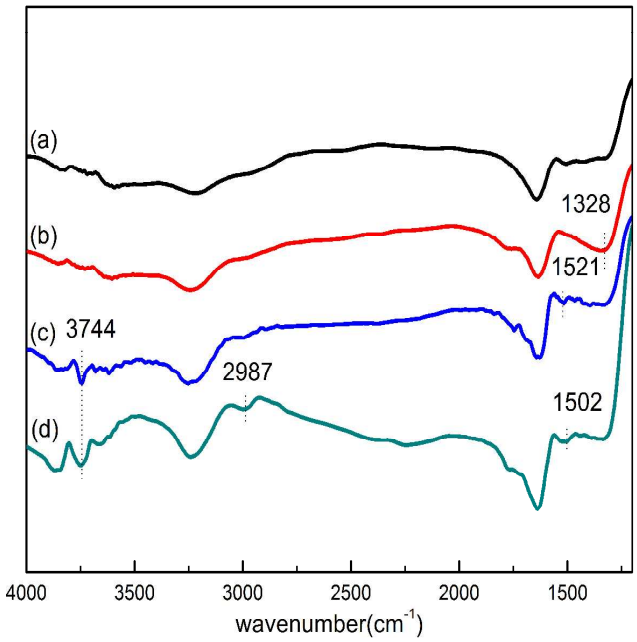

Fig.2 FT-IR spectra of: (a) AC, (b) AC-NO_2, (c) AC-NH_2, (d) AC-NHN.

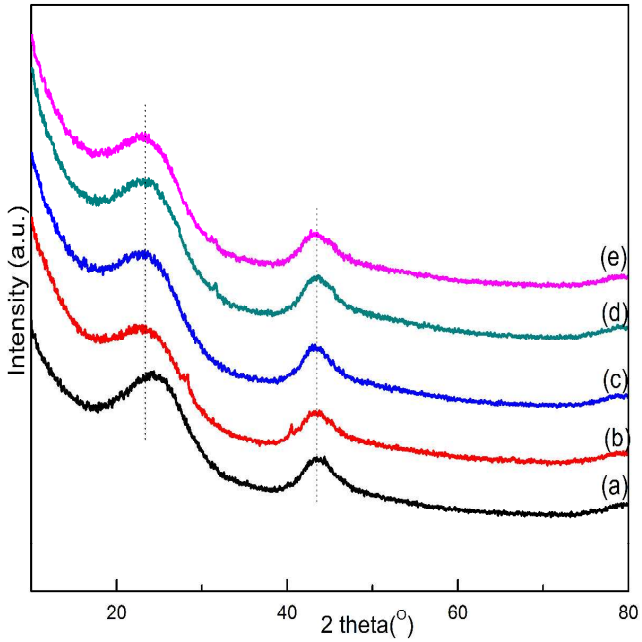

Fig.3 X-ray diffraction patterns of (a) the support AC and the fresh catalysts (b) Ru/AC, (c) Ru/AC-NO_2, (d) Ru/AC-NH_2 and (e) Ru/AC-NHN.

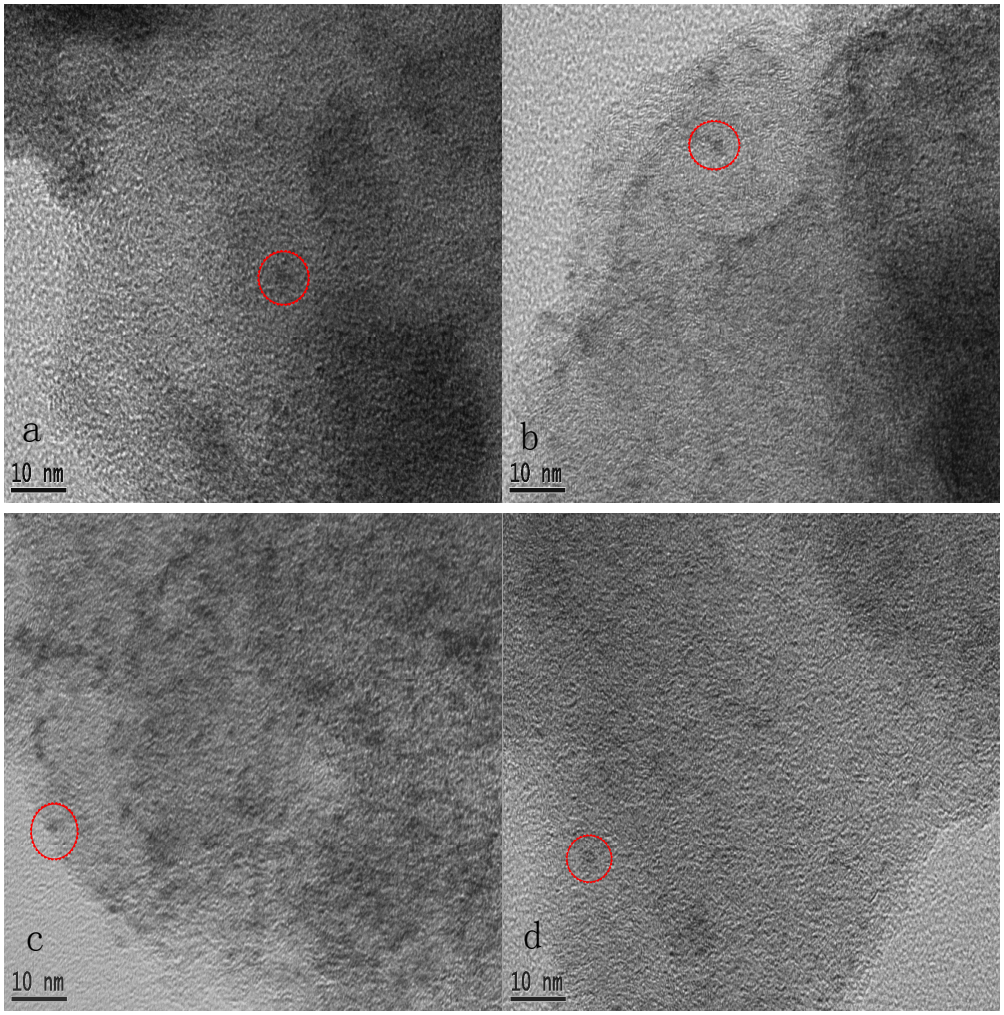

Fig.4 TEM images of the fresh catalysts: (a) Ru/AC, (b) Ru/AC-NO_2, (c) Ru/AC-NH_2, and (d) Ru/AC-NHN.

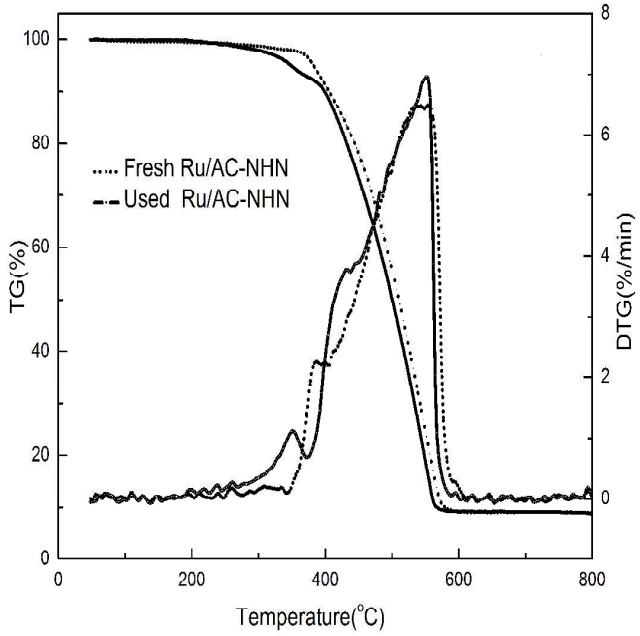

Fig.5 TGA curves of the fresh and used catalysts of Ru/AC-NHN.

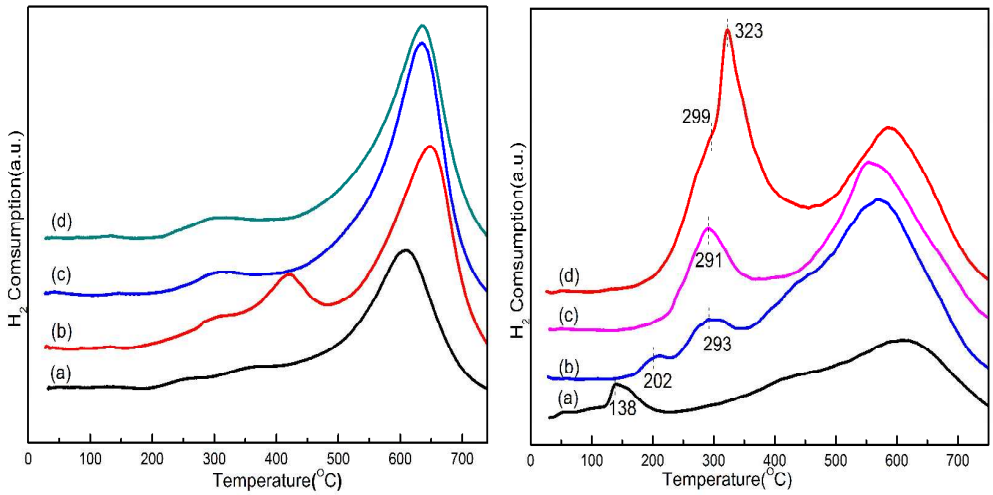

Fig.6 TPR profiles of the supports: (a) AC, (b) AC-NH_2, (c) AC-NO_2, (d) AC-NHN and the catalysts: (a) Ru/AC, (b) Ru/NH_2, (c) Ru/AC-NHN, and (d) Ru/AC-NO_2.

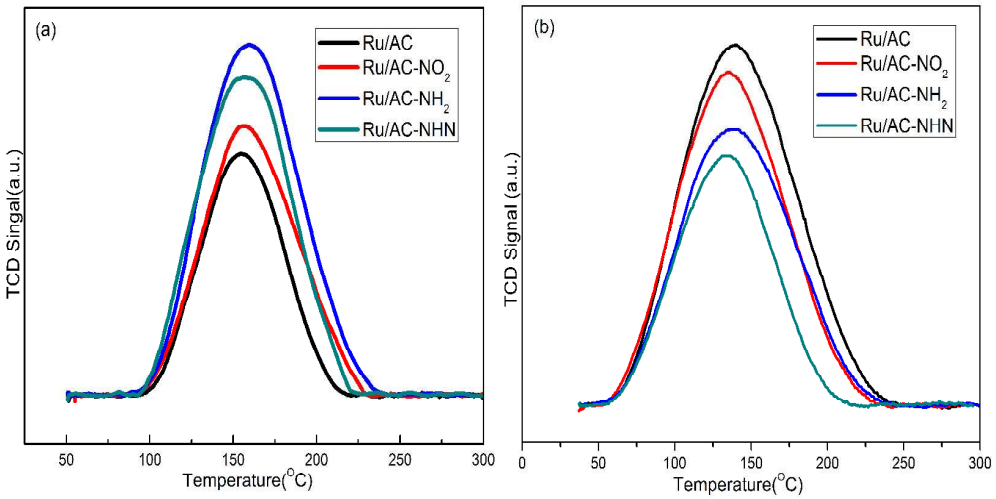

Fig.7 TPD evolution profiles of Ru-based catalysts: (a) HCl- and (b) C_2H_3Cl-.